Premixed, turbulent combustion of axisymmetric sudden expansion flows

S. A. Ahmed and A. S. Nejad
Advanced Propulsion Division, Aero Propulsion and Power Directorate,
Wright-Patterson AFB, Ohio, USA

Velocity and low-frequency combustor pressure oscillations have been measured in a ramjet dump combustor model. The mean and root mean square (rms) values of the turbulent velocity field were obtained using a two-component laser Doppler velocimeter (LDV) system operating in the backscatter mode. Reacting flow data were obtained for premixed propane and air, while isothermal results were collected after replacing the propane with nitrogen. The velocity data indicated substantial differences between the two cases. Combustor pressure oscillation data were also obtained. The intensity and frequency of the oscillations were found to be dependent on the inlet velocity, combustor length, and equivalence ratio. Results showed that pressure oscillations were controlled by both vortex kinematics in the combustor and acoustic response of the inlet section.

Keywords: turbulent combustion; premixed, experimental, axisymmetric sudden expansion

Introduction

Turbulent sudden expansion flows are of significant theoretical and practical importance. Despite the fact that such flows have been the subject of extensive analytical and experimental studies for decades, many issues are still unresolved. For example, because of the complexity of the flowfield and the associated difficulties with measurements, detailed information on reacting sudden expansion flows are very limited. As a result, development and evaluation of analytical models of the flowfield, especially for confined turbulent recirculating flow configurations, have been hampered by the lack of reliable and detailed experimental data. Therefore, in order to develop these numerical codes such as the k-ε model to become general (i.e., applicable to more than a limited range of simple configurations), reliable and well-documented experimental data are a must. Therefore, the objective of the current study is to obtain a credible and detailed experimental database and to help in the understanding of the behavior of such flows. There are limited data available for geometries that parallel the current study. However, in one way or another, the data lack detail and accuracy (i.e., initial conditions or resolution) or do not represent a realistic geometry or combustor operating condition. Several researchers have reported data for geometries that may complement the current study. Flow characteristics of interest that were examined included the velocity field characteristics, the length of the corner recirculation zone (CRZ), and the pressure distribution. The most recent studies relevant to the present one are discussed in the following paragraphs.

Pitz and Daily[1] investigated reacting flow behind a step in a rectangular duct with a 2:1 area ratio. They reported that the presence of reaction (equivalence ratio = 0.57) reduced the length of the CRZ by 20–30 percent. Turbulence parameters were not of prime interest and were not heavily discussed. The limited data that were plotted indicated combustion had an insignificant effect on turbulent kinetic energy (TKE).

Address reprint requests to Dr. S. A. Ahmed at the Advanced Propulsion Division, Aero Propulsion and Power Directorate, Wright-Patterson AFB, OH 45433-6563, USA.

Received 18 December 1990; accepted 15 June 1991

El Banhawy et al.[2] studied reacting flows with equivalence ratios ranging from 0.77–0.95 and expansion area ratios of 2.0 and 4.0 in a coaxial dump combustor. They observed a CRZ extending approximately three step heights. The reported value was less than half of the commonly observed value in nonreacting flows and 30–40 percent lower than the documented results of Pitz and Daily.[1]

Stevenson et al.[3] reviewed relevant results and made measurements in an axisymmetric sudden expansion combustor with an equivalence ratio of 0.28, using nonpremixed flow conditions. They found that the reaction shortened the CRZ by approximately 15 percent, increased the maximum backflow velocity and the axial TKE on the centerline while reducing TKE elsewhere. In agreement with prior investigators, they reported the significance of axial pressure gradient on CRZ length in nonreacting flows, indicating that this parameter needs to be isolated and monitored closely before considering the effects of combustion on the behavior of the CRZ.

Smith and Giel[4] evaluated the characteristics of a coaxial hydrogen-fueled confined burner with an equivalence ratio of 0.14 and a diameter ratio of approximately 2.5:1. The central air velocity was 102.1 m/s (335 ft/s), and the hydrogen flow in the annulus was 0.91 m/s (3 ft/s), which was so low that it did not prevent the flow from exhibiting a recirculation pattern near the wall region. Reaction and heat release caused a significant change in the axial pressure distribution and the length of the wall recirculation, i.e., decreasing axial pressure gradient and doubling the length of the recirculation zone. Similar studies by Chris[5] showed no change in wall recirculation length when the diameter ratio was 10:1. The maximum TKE showed little change with reaction, although the peak value occurred farther downstream for the reacting case.

Other investigators such as Waugh[6] investigated oscillatory operation in ramjet combustors over a broad range of conditions. These oscillations are generally grouped into three broad classes that can be correlated with the acoustic properties of the combustor. These are high-frequency oscillations greater than 1,500 Hz, low-frequency oscillations 500–1,500 Hz, and very low-frequency oscillations that have frequencies below the first longitudinal acoustic mode of the combustor. In some instances, occurrence of very low-frequency oscillations of small

amplitudes can be detrimental to the operation of the ramjet engine. This is a result of the pressure excursion propagating upstream into the diffuser, which may cause expulsion of the inlet shock thus drastically reducing the engine thrust and efficiency. In many cases, the very low-frequency oscillations are close to the first longitudinal combustor mode. Since combustion typically occurs over the first 25–75 percent of the combustor length, energy release is not considered to be the most effective way of exciting the first longitudinal mode. Burning rate is sensitive to pressure and temperature fluctuations in the chamber that can be coupled to mass flow fluctuations. Therefore, the primary destabilizing mechanisms are oscillations of fuel and air mass flow rates and the time lag between the entry of the reactants and energy release due to combustion. Other phenomena identified as possible mechanisms for ramjet oscillations include vortex shedding generated at the dump plane, as reported by Flandro and Jacobs[7] and Dunlap,[8] periodic distortion of the combustion zone by vortices generated at the inlet,[9] and the upstream propagation of entropy waves that are reflected from the exhaust nozzle.[10]

Early evidence of the role of vortical structures during unstable operation was first noted by Rogers and Marble.[11] They proposed a general mechanism that describes the energy exchange between the oscillating pressure field and the flame zone. Similar pulsating combustion phenomena were also reported by Smith and Zukoski[12] in a rearward-facing step experiment.

Recent experimental investigations[12–17] support the hypothesis that low-frequency instabilities in dump combustors result from similar interactions between the flame zone and the longitudinal acoustic modes of the whole system.

The previously mentioned studies show the nature of combusting flows. However, in quantification of the flowfield of interest to the ramjets, the experiment data are lacking. Thus, there is a need for the present work, which is a part of an ongoing detailed study of a typical ramjet configuration from isothermal to a reacting high speed flow. This should provide the necessary experimental data for computational fluid dynamics development and its validation.

Experimental set up

Water-cooled combustor

Figure 1 shows the test section in detail. The combustor consisted of two major sections: the inlet assembly and the combustor chamber and exhaust nozzle. The inlet assembly consisted of a settling chamber, inlet pipe, the associated temperature and pressure instrumentation, and the stainless steel swirler housing. The combustor section consisted of a water-cooled pipe that terminated in an exhauster used to simulate high-altitude conditions.

This modular design allowed optical access for two-dimensional LDV measurements while preserving the integrity of the combustor flowfield. One of the unique features of this design was the ability to position the dump plane relative to the combustor measurement station. Other special features included a 38 × 38 mm (1.5 × 1.5 in) flat quartz window installed in the inlet pipe for measurements upstream of the swirler. Inlet flow disturbances were eliminated when measurements in the combustor section were performed, by replacing the quartz window with a plug having the same radius of curvature as the inlet pipe. Similarly, on the combustor section, an air-cooled quartz window used for LDV measurements was assembled on a flexible mount (combination of springs and bolts) to allow for the differential thermal expansion of the quartz and the metal surfaces as shown in Figure 1.

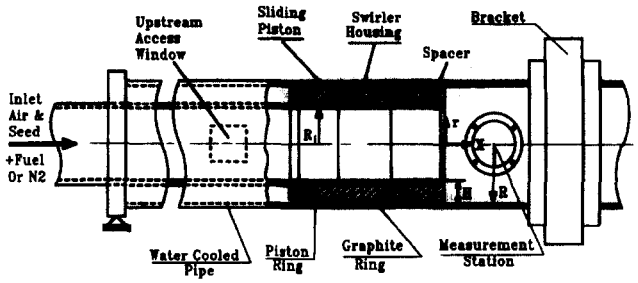

Figure 1 Schematic of the dump combustor model

The water-cooled stainless steel combustor was conceptually and physically identical to the Plexiglas rig used earlier by Favaloro et al.[18] However, new design methodologies were implemented to allow stable and continuous combustor operation over long periods of time. For the current experiment, four side-injector tubes (90° apart, 1.52 mm [0.06 in] diameter ports) were used for premixed studies. Injector ports were located 12.7 mm (0.5 in) from the 101.6-mm (4.0 in) inlet pipe centerline just downstream of the 50.8-mm (2.0 in) diameter orifice plate. The ports were aligned to point downstream. This configuration provided premixed conditions and attenuated flow oscillations, while eliminating flashback over the range of operating conditions reported here. To ignite the fuel/air mixture, two spark plugs, flush mounted 180° apart in the step face, were used.

Instrumentation

Both nonintrusive and conventional techniques were used in the present study. For the velocity and turbulence measurements, a two-color, four-beam backscatter TSI standard LDV system with some in-house modifications was used. The details of the system were reported earlier by Favaloro et al.[18] Seeding was accomplished via a reaction of $TiCl_4$ and H_2O, producing TiO_2 particles of approximately 1 μm in diameter.

Temperature measurements from low to moderately high temperature ranges (i.e., the inlet air, water jacket, fuel,

Notation

F	Frequency (Hz)
H	Step height, 1″ (25.4 mm)
L	Length of combustor
r	Radial coordinate
R	Combustor radius, 3″ (76.2 mm)
U, W	Time mean axial and tangential velocities
u', w'	Axial and tangential rms turbulent velocities
$\overline{uw}$	Reynolds shear stress ($U - W$ plane)
X	Axial coordinate

Greek symbols

ϕ	Equivalence ratio
θ	Axial momentum thickness

Subscripts

o	Inlet condition value
ref	Inlet centerline values

combustor outer wall, and exhauster temperatures) were obtained by using type K thermocouples. Type R thermocouples were used to measure combustor temperature profiles, which are usually much higher.

Wall pressure measurements were made by using thin-film pressure transducers (CEC 55000). For dynamic pressure measurements, two high-frequency Kulite pressure transducers were installed in the inlet pipe (upstream of the dump plane) and the combustor chamber (on the opposite side to the quartz window and along the laser axis). A Nicolet Scientific Corporation Model 660-A dual-channel FFT analyzer was used to obtain spectral densities of pressure signals. For all spectral analysis, the sampling rate was 2.56 times the maximum frequency for dual-channel analysis. For most of the data, 150 averages and a 500-Hz frequency range were selected. Each block of data contained 400 samples, which resulted in a resolution of 1.25 Hz.

A Yokogawa vortex flowmeter Model YF100 was used to measure inlet volume flow rate. A Flow Technology Model FT-08AER1-GEA-1 turbine type flowmeter was used to measure the fuel flow rate. A Neff System 470 data acquisition system was used to calculate, display, and monitor all pertinent flow parameters such as mass flow rates, temperatures, and pressures.

Experimental results

The control parameters chosen in operating the water-cooled combustor were the upstream mean velocity U_{ref}, L/H, and ϕ. Table 1 shows the operating conditions chosen for the instability studies. The results were accomplished through detailed fluctuating pressure measurements. In addition, some velocity measurements were taken for various combustor lengths to check velocity-pressure correlations. For most of these operating conditions, periodic oscillation in the pressure was noted and recorded. The details of the results are discussed in the following sections. The case of $U_{ref} = 18.25$ m/s (60 ft/s) and $\phi = 0.56$ was selected as the baseline testing to examine velocity and wall static pressure measurements in depth.

Mean flow results

Initial conditions. Figure 2 shows a typical inlet velocity profile upstream of the dump plane. The plots show variations of axial velocity and normalized rms velocity profiles across the inlet pipe that are similar to fully developed pipe flow data. It is worth noting that the inlet flow is smooth and symmetric, indicating a well-controlled combustor inlet flow. The turbulence level at the center was approximately 5 percent. This increased away from the centerline and reached a maximum value of 9.5 percent in the vicinity of the wall, which agrees with previous isothermal flow results reported by Samimy et al.[19] taken in a similar Plexiglas rig.

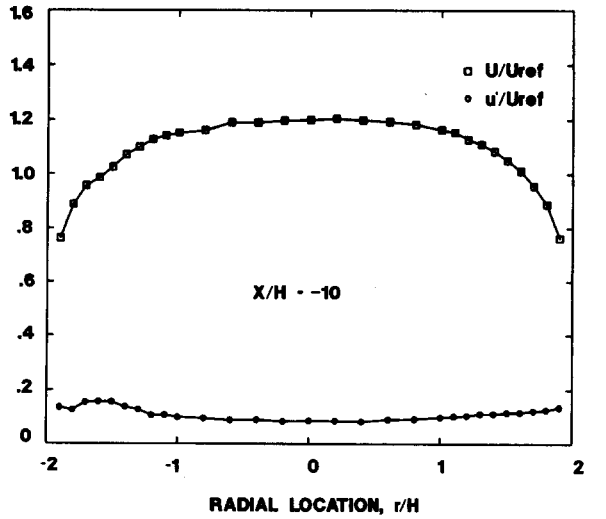

Figure 2 Upstream inlet conditions

Mean velocity results. One case was selected only for detailed velocity measurements with a reference velocity of 18.25 m/s (60 ft/s), corresponding to a Reynolds number of 1.18×10^5 based on inlet velocity and pipe diameter. The axial distance from the center of the windows and the dump plane, X, was increased from $X/H = 0.38$ to $X/H = 24$ to allow for velocity measurements at different axial locations (i.e., $X/H = 0.38$, 1, 2, 3, 4, 5, 6, 8, 10, 12, 15, 18, and 24). However, only the results of four axial locations are reported here to illustrate the flowfield characteristics of reacting and nonreacting cases. These representative axial locations are $X/H = 0.38$, 3, 6, and 12. Other data in tabulated formats are available from the authors on request. Figures 3–6 display the substantial differences between the hot and cold flow cases and illustrate the significant effects of combustion on the flowfield characteristics. Similar results were reported earlier by other investigators such as El-Banhawy et al.[2] and Stevenson et al.[3] Figure 3 shows the evolution of axial velocity profiles that showed insignificant differences between the cold and hot flow in the central region $0 < r/H < \pm 2$, especially in the near field. Differences were noted in the shear layer around the $r/H \approx 2$, which grows in size with increasing axial distance. This demonstrates that in the near field, combustion is mostly limited to the shear layer. Away from the dump plane (i.e., $X/H > 6$), the shear layer increased in thickness tremendously to the point of occupying the entire cavity of the combustor. In the far field ($X/H \geq 12$), due to combustion and heat release, the velocity is substantially higher and the profile is more uniform, indicating flow recovery to fully developed pipe flow in a short distance as compared with the nonreacting case. Tangential velocity measurements showed

Table 1 Operating conditions for the instability studies

ϕ	L/H	U_{ref} (ft/s)						
0.6	28.5	31.21	44.8	61.37	75.47	88.82	104.67	120.35
0.6	40.5	31.52	44.81	60.65	76.77	92.33	105.31	120.41
0.6	52.5	31.09	45.22	61.52	75.72	88.21	106.41	120.88
0.65	28.5	30	45	60	72	92.14	106.97	118.67
0.65	40.5	30	45	60	75	90.86	105.72	120.73
0.65	52.5	30	45	60	75	89.81	105.58	119.15
0.70	28.5	30.82	40.8	60.5	74.26	88.77	104.14	118.22
0.70	40.5	31.01	45.63	61.30	74.90	90.93	107.17	119.46
0.70	52.5	30.35	45.58	61.43	75.16	90.10	105.78	119.48

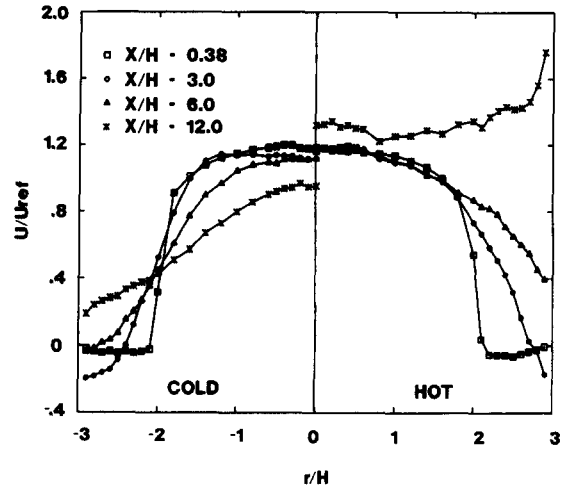

Figure 3 Evolution of axial velocity profiles

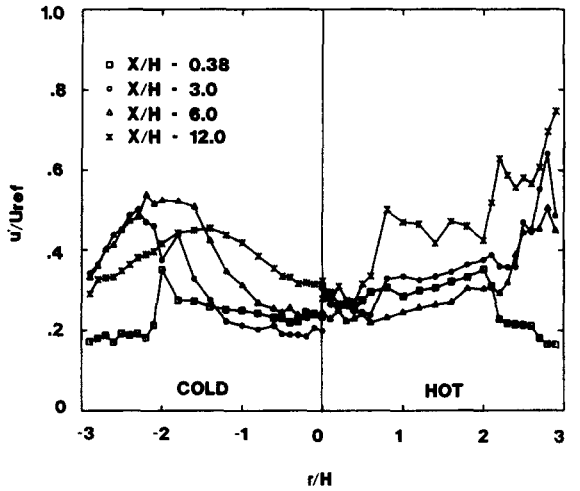

Figure 4 Evolution of axial turbulent velocity, $\phi = 0.65$

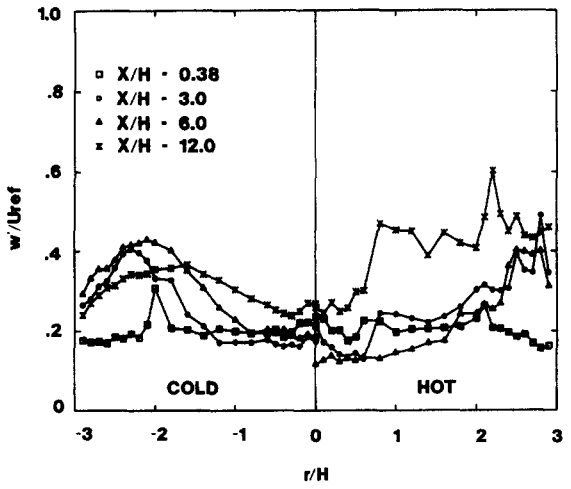

Figure 5 Evolution of tangential turbulent velocity, $\phi = 0.65$

insignificant values scattered around zero, and for brevity they are not shown.

Figures 4 and 5 show the corresponding radial distributions of the axial and tangential rms velocities. In general, the axial turbulence intensities are larger than their corresponding tangential values in both cases of hot and cold flows. Also, the maximum intensities of both velocity components occurred at the same radial location. It appears that the maxima in the hot flow case are located closer to the wall, suggesting the movement of the mixing layer toward the walls (i.e., shorter recirculation region length, which is in agreement with the results of Figure 3). It is obvious that the turbulence level increased due to combustion in both directions except at $X/H = 6$. In spite of this, the local turbulence intensities, u'/U and w'/U, are smaller in the hot case than their corresponding cold flow values. This is in agreement with some of the earlier results of El-Banhawy et al.[2]

Contour plots are usually presented to help with the interpretation of the measurements and to provide a better picture of the flowfield. Valuable information such as regions of maximum or minimum and zero lines can be easily identified. For example, contours of the normalized axial velocities are shown in Figure 6. The reverse flow boundaries defined by $U/U_{ref} = 0.0$ are shown. In the presence of combustion, the length of the corner recirculation zone decreased 44 percent from 6.7–3.75 step heights. A close examination of the plots show that, in spite of the reduction in the corner recirculation region length, the flow inside the bubble is more active as demonstrated by higher values of negative velocities. The contour lines show substantial increase in axial velocity across the combustor downstream of $X/H = 10$. This is an indication that combustion has taken place across the entire cross section of the combustor at that axial location and also downstream of it.

Instability results

Several cases summarized in Table 1 were investigated to examine the effects of combustor geometry and flow parameters on combustion instability. Although the equivalence ratio of the lean blow-off limit was ≤ 0.51, all experiments were conducted at higher equivalence ratios ($\phi \geq 0.60$) to avoid flashback and combustion oscillations associated with operating near lean blow-off limit. Here, the main objective was to characterize the pressure oscillations of the flowfield for different combustor lengths and different inlet flow velocities. Depending on the operating conditions, higher harmonics or subharmonics may appear and become quite intense. Of course, these different spectral components contribute to significant cyclic variations in the amplitude of the oscillations.

Power spectral analysis of the transducer's output for zero velocity flow did not reveal any distinct frequencies in the range of interest (< 200 Hz). This was done in order to check for any ground loops or electronic noise of any type. However, lower frequencies (17.5, 60, and 160 Hz) were recorded in the cold flow case of $U_{ref} = 32$ m/s (105 ft/s). The 60 Hz frequency was slightly more dominant and narrower than the other two frequencies. For free shear layers generated from an initial

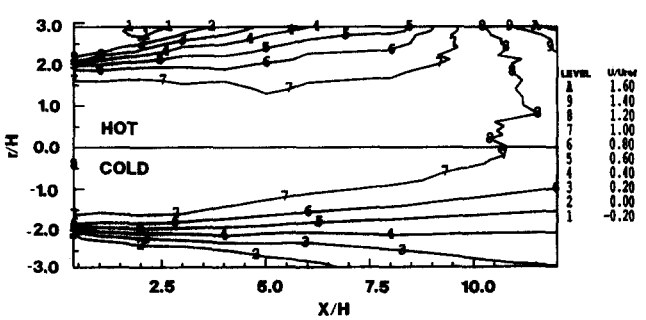

Figure 6 Contours of mean axial velocity, $\phi = 0.65$

boundary layer with a uniform momentum thickness, such as the present configuration, linear stability theory[20] predicts the strongest roll-up frequency to be approximately 220 Hz (i.e., $F = 0.017U_{ref}/\theta_o$ where U_{ref} and θ_o are the inlet velocity and momentum thickness, which was estimated to be 2.9 mm, 0.11 in). On the other hand, the range of the first acoustic mode of the combustor (i.e., L varied between 0.87 and 1.48 m, 34.25 and 58.25 in) is 120–200 Hz. Similarly, the longitudinal acoustic mode of the inlet pipe is 58.5 Hz considering the total length of the inlet pipe, which is approximately 3 m (118.1 in). Apparently, the recorded frequency of 60 Hz is excited by the longitudinal acoustic mode of the inlet pipe. Generally speaking, the system acoustics play an important role in determining the nature of the instability. However, for most of the operating conditions, the results indicate that the instability mechanism cannot be purely acoustic but is rather a combination of the system acoustics and the flow instabilities, which is mainly dominated by vortex shedding. One can see how complicated the flow has become when combustion is introduced. Figures 7 and 8 reflect this fact.

Figure 7 shows the differences between the two signals recorded by the pressure transducers for $\phi = 0.7$, $\phi = 0$, and $U_{ref} = 32$ m/s (105 ft/s). Note the presence of higher frequency harmonics recorded in the inlet (160 and 208 Hz) and how they were amplitude modulated showing wider band.

Figure 8 illustrates the effect of U_{ref} on the coherent output power of both transducer signals (i.e., it was chosen to eliminate the uncorrelated events). The plots clearly show the monotonic increase of the oscillation frequency with increasing U_{ref} for the case of $\phi = 0.7$ and $L/H = 40.5$. These frequencies were recorded and the results are summarized in Table 2. Mostly, these frequencies did not match the inlet acoustic resonance frequency. Therefore, it is worthwhile to examine the relationship between the inlet velocity and frequency as a function of combustor length for a fixed value of ϕ. It is obvious when the velocity is increased, the frequency increases approximately in a linear fashion as shown in Figure 9, which is in agreement with the linear stability theory results. This suggests that the frequency is closely related to the vortex dynamics in the reaction zone. The effect of the combustor length is also obvious since the frequency of oscillation increases as combustor length decreases for the same values of ϕ and U_{ref} as shown in Table 2. In other words, this further suggests that there is a relationship between the pressure oscillation frequency and the combustor acoustic mode. Figure 10 is generated by using the data of Figure 9 in addition to replotting $1/F$ *versus* L/U_{ref} (to combine the two dominant variables controlling the frequency value). It shows that most of the data points fall on a straight line. A linear regression through these points has a slope of 0.095 and an intercept of 9.2 ms. The intercept time of 9.2 ms closely corresponds to the round-trip travel time of a pressure wave generated in the combustor and reflected from upstream boundaries to return to the combustor. This corresponds to a frequency of 55.5 Hz, which is approximately equal to the calculated acoustic mode frequency of 58.5 Hz. Since L/U_{ref} is approximately equal to the vortex lifetime (i.e., assuming the vortex breaks up when it impinges on the exit nozzle; in reality, for long combustors the vortex might disperse before reaching the nozzle), the time period appears to be the sum of the vortex characteristic time L/U_{ref} and the characteristic inlet acoustic time. In other words, the vortex lifetime is associated with the characteristic convection time in the combustor while the round-trip time characterizes the acoustic response of the inlet. In summary, combustor instability frequencies are determined by both vortex dynamics and the inlet acoustic response time.

The distribution of total rms of the pressure signal for the

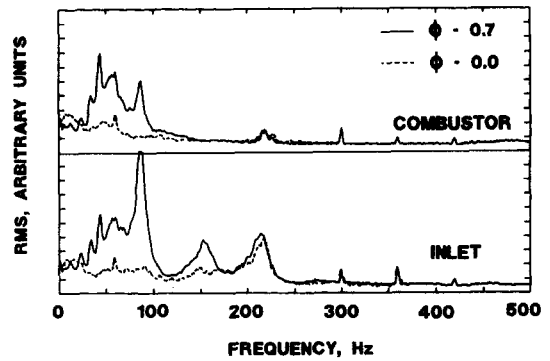

Figure 7 Power spectra of pressure oscillations $L/H = 52.5$, $U_{ref} = 32$ m/s

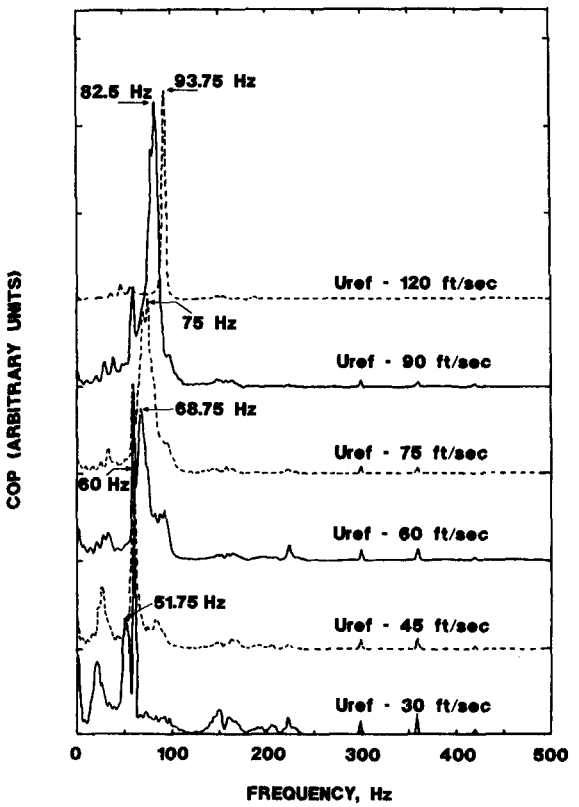

Figure 8 Coherent output power spectra

Table 2 Summary of the instability results for $\phi = 0.7$

L/H				F (Hz)			
28.5	53.75	60	76.25	80	90	97.5	100
40.5	51.75	60	68.75	75	82.5	88.75	93.75
52.5	47.5	53.75	61.25	67.5	76.25	86.25	—
U_{ref}	30	45	60	75	90	105	120

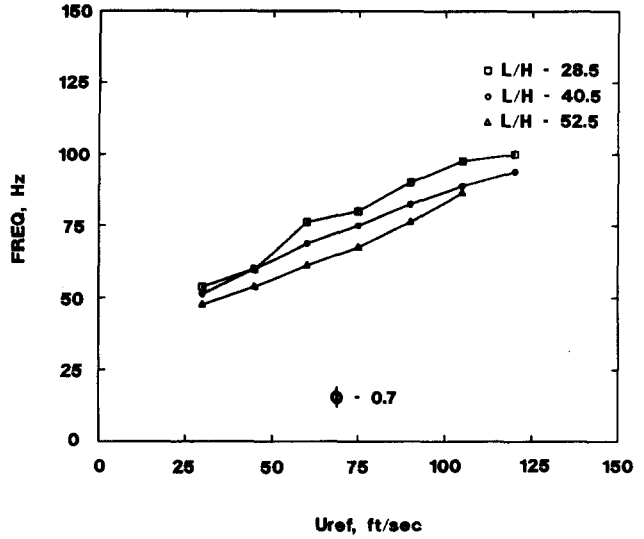

Figure 9 Pressure oscillation frequencies *versus* inlet velocity, $\phi = 0.7$

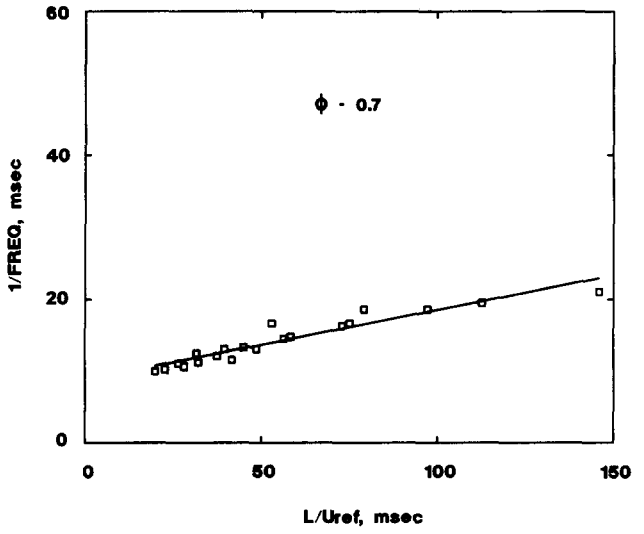

Figure 10 Oscillation period *versus* characteristic flow residence time, $\phi = 0.7$

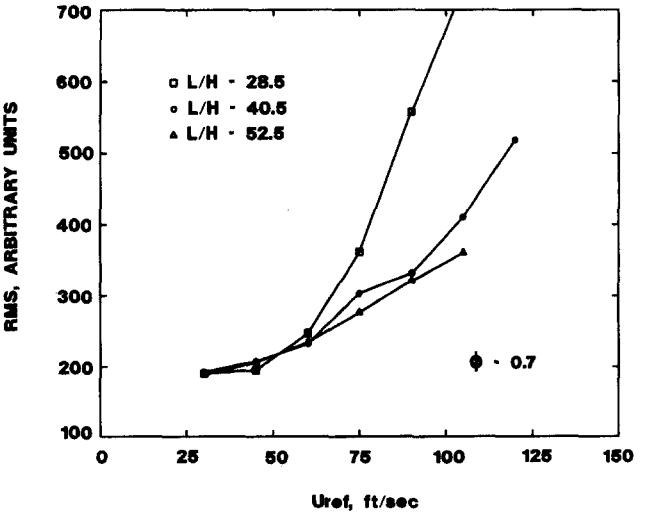

Figure 11 Turbulent pressure rms values *versus* inlet velocity, $\phi = 0.7$

combustion case is significantly higher than the corresponding isothermal flow case. All data show an increased rms value when either the upstream reference velocity or ϕ is increased or the combustor length is decreased. For brevity, only the results of $\phi = 0.7$ are presented (Figure 11).

Summary and conclusions

A detailed experimental investigation was carried out to determine the effects of combustion on the flowfield characteristics of a model ramjet engine. The study also described the low-frequency vortex-driven pulsating combustion modes and the nature of the pressure oscillations observed in the flowfield. The results showed the significant effects of combustion on the development of sudden expansion dump combustor flowfield. For example, the mixing layer, inferred by velocity measurements, shifted toward the combustor wall. As a result, corner recirculation region length decreased by approximately 44 percent. This was accompanied by a much faster flow recovery, i.e., flat velocity and turbulence profiles not far from the dump plane.

Systematic manipulation of the combustion instability frequencies showed that the resonant period of the oscillation is determined by the sum of the vortex convection in the combustor and the acoustic feedback time of the inlet. For shorter combustors, the oscillations were more intense and their frequencies were higher. Similar effects were noticed when the reference inlet velocity was increased.

Further detailed and refined data should become available in the near future. Future studies will include the effects of combustion on the flowfield characteristics of combustors with inlet swirling flows.

Acknowledgments

The authors would like to thank John Hojnacki and Charlie Smith for their continuous support. Special thanks goes to the Air Force Office of Scientific Research and to Dr. Julian Tishkoff for providing sponsorship.

References

1 Pitz, R. W., and Daily, J. W. Combustion in a turbulent mixing layer formed at a rearward-facing step. *AIAA Journal*, 1983, **21**, 1565–1570

2 El Banhawy, Y., Sivasegaram, S., and Whitelaw, J. H. Premixed turbulent combustion of a sudden expansion flow. *Combustion and Flame*, 1983, **50**, 153–165

3 Stevenson, W. H., Thompson, H. D., and Gould, R. D. Laser velocity measurements and analysis in turbulent flows with combustion. Parts I and II. AFWAL-TR-82-2076, 1983

4 Smith, G. D., Giel, T. V., and Catalano, C. G. Measurements of reactive recirculating jet mixing in a combustor. *AIAA Journal*, 1983, **21**, 270–276

5 Chris, D. E. An experimental investigation of ducted reactive turbulent jet mixing with recirculation. AECD-TR-77-56, AFOSR-TR-77-0749, ADA 044110, 1977

6 Waugh, R. C. Ramjet combustor instability investigation literature survey and preliminary design study. AFWAL-TR-83-2056, Vol. I, United Technologies Chemical Systems, San Jose, CA, USA, September, 1983

7 Flandro, G. A., and Jacobs, H. R. Vortex generated sound in cavities in aeroacoustic: Jet and combustion noise: Duct acoustic. Nagamatse, H. (ed). *Progress in Astronautics and Aeronautics*, AIAA, **37**, 1975

8 Dunlap, R. Internal flowfield investigation. AFRPL-TR-85-079 United Technologies, Chemical System Division, San Jose, CA, USA, 1985

9 Marble, F. E. Some comments concerning relationship between chemical reactors in vortex structure and unsteady combustion. *Presented at the ONR/AFOSR Workshop on Mechanism of Instability in Liquid Fueled Ramjets*, Atlanta, GA, March 1983

10 Waugh, R. C., and Brown, R. S. Entropy wave instability—comparison of data and analysis. *Presented at the 21st JANNAF Combustion Meeting*, Laurel, MD, October 1984

11 Rogers, D. E., and Marble, F. E. A mechanism for high frequency oscillations in ramjet combustors and afterburners. *Jet Propulsion*, 1956, **26**, 456–462

12 Smith, D. A., and Zukoski, E. E. Combustion instability sustained by unsteady vortex combustion. *21st Joint Propulsion Conference*, Monterey, CA, USA, Paper No. 1248, 1985

13 Keller, J. O., and Daily, J. W. The effects of highly exothermic chemical reaction on a two-dimensional mixing layer. *AIAA Journal*, 1985, **23**, 1937–1945

14 Poinsot, T., Trouve, A., Veynante, D., Candel, S. M., and Esposito, E. Vortex driven acoustically coupled combustion instability. *J. Fluid Mech.*, 1987, **177**, 265–292

15 Sterling, J. D., and Zukoski, E. E. Longitudinal mode combustion instabilities in a dump combustor. 25th Aerospace Sciences Meeting, Reno, NV, No. 0220, 1987

16 Hedge, U. G., Reuter, D., Zinn, B. T., and Daniel, B. R. Fluid mechanically coupled combustion instabilities in ramjet combustors. 25th Aerospace Sciences Meeting, Reno, NV, No. 0216, 1987

17 Langhorne, P. J. Reheat buzz: An acoustically coupled combustion instability. Part I. Experiment. *J. Fluid Mech.*, 1988, **193**, 417–443

18 Favaloro, S. C., Nejad, A. S., Ahmed, S. A., Miller, T., and Vanka, S. P. An experimental and computational investigation of isothermal swirling flow in an axisymmetric dump combustor. *AIAA* Paper No. 89-0620, 1989

19 Samimy, M., Nejad, A. S., Langenfeld, C. A., and Favaloro, S. C. Oscillatory behavior of swirling flows in a dump combustor. *AIAA* Paper No. 88-189, 1988

20 Michalke, A. On spatially growing distributions in an inviscid shear layer. *J. Fluid Mech.*, 1965, **23**, 521–544